Available online at www.sciencedirect.com
SCIENCE DIRECT®
PERGAMON
International Journal of Heat and Mass Transfer 46 (2003) 3397–3409
International Journal of HEAT and MASS TRANSFER
www.elsevier.com/locate/ijhmt

# A methodology to work on geometrically complex heat transfer systems: the cases of heat conduction through composite slabs

Wataru Nakayama *

*ThermTech International, 920-7 Higashi Koiso, Oh-Iso Machi, Kanagawa 255-0004, Japan*

Received 1 July 2002; received in revised form 19 February 2003

**Abstract**

Geometrical complexity considered in the present study is characterized by a large degree of freedom in placement of constituents in a composite system. The constituent sizes are not negligibly small compared to the system's expanse, so approximations of their configurations and placement patterns by some simple equivalents are not feasible. Numerical analysis is a means to estimate heat transfer performance of the system, but a strategy is required to navigate through a vast number of possible constituent patterns to find ones that produce higher heat transfer performance. In the proposed methodology the constituent pattern is captured as a two-dimensional mosaic image of solid cells embedded in a substrate. On an image assumed as a starter, the singular-value decomposition (SVD) analysis is performed to find its (SVD) building block elements. By shuffling the building block elements variants of the starter image are created. Heat transfer analysis is performed on sample systems that are picked up from the ensemble of variants. Using the Taguchi method and through a genetic algorithm-type reasoning, those element arrangements that do not significantly affect the heat transfer performance are weeded out. The methodology is demonstrated on the cases of heat conduction through composite slabs.
© 2003 Elsevier Science Ltd. All rights reserved.

*Keywords:* Singular-value decomposition analysis; Composite materials; Heat conduction; Optimization; Search algorithms; Geometric complexity

## 1. Introduction

The subject of the present study is heat transfer in geometrically complex systems. The 'geometric complexity' implies a wide range of length scales involved in the system's organization and the absence or disruption of regularity in placement of structural components within the system. Where irregularities have much finer scales than the system's dimension, they can be characterized by certain statistical measures. Then, the effects of such microscopic irregularities or aberrations on heat transfer are captured in terms of the statistical measures. For example, heat conduction through composite materials has been studied by a number of investigators in the past, and the equations based on the concept of ensemble averaging are now developed [1]. In actual analysis, microscopic fibrous or granular inclusions in composite material are modeled by particles of well-defined configuration (rod or sphere). Further, in order to make the analysis tractable, their spatial placement is often projected first onto a regular pattern, then, deviations from the base positions are assumed using a distribution function. Such an approach starting from a homogenous model works better, as the inclusions become minuscule and more populous.

In another recent development to deal with geometrically complex systems, the first step is the assumption of a simple elementary geometry, then, the element configuration is multiplied changing the size of offspring configurations in a stepwise fashion [2–4]. Geometric

* Tel./fax: +81-463-61-4246.
*E-mail address:* watnakayama@aol.com (W. Nakayama).

0017-9310/03/$ - see front matter © 2003 Elsevier Science Ltd. All rights reserved.
doi:10.1016/S0017-9310(03)00136-4

**Nomenclature**

| | |
|---|---|
| $A$ | geometric parameter for placement of $X_i$- or $x_i$-elements |
| $B$ | geometric parameter for placement of $Y_j$- or $y_j$-elements |
| $\mathbf{I}$ | unity matrix |
| $K$ | number of eigenvalues |
| $k_0$ | thermal conductivity of open cell |
| $k_1$ | thermal conductivity of solid cell |
| $k_{e,i}$ | equivalent thermal conductivity (non-dimensional), $i$ being $x$ or $y$ |
| $L_i$ | slab length, $i$ being $x$ or $y$ |
| $m$ | maximum number of rows in $\mathbf{S}$ |
| $n$ | maximum number of columns in $\mathbf{S}$ |
| $Q_i$ | heat flow rate through a slab having a cross-sectional area $L_j \times 1$; subscript $i$ indicating the direction of heat flow ($x$ or $y$), and $j$ (to $L_j$) the direction normal to that of $i$ ($y$ or $x$) |
| $\mathbf{S}$ | matrix of a component placement pattern |
| $\mathbf{S}^{\mathrm{T}}$ | transpose of $\mathbf{S}$ |
| $S_Z$ | effect of parameter $Z$ on heat transfer performance, $Z$ being any of geometric parameters ($A$–$B_2$) |
| $T$ | non-dimensional temperature (to the scale of $\Delta T$) |
| $\Delta T$ | temperature difference between the opposite faces of the slab |
| $\mathbf{U}$ | matrix composed of left-singular vectors |
| $\mathbf{u}^{(k)}$ | $k$th left-singular column vector |
| $u_{i,k}$ | $(i,k)$ element of $\mathbf{U}$ |
| $\mathbf{V}$ | matrix composed of right-singular vectors |
| $\mathbf{V}^{\mathrm{T}}$ | transpose of $\mathbf{V}$ |
| $\mathbf{v}^{(k)}$ | $k$th right-singular column vector |
| $X_i$ | row element group |
| $x$ | co-ordinate axis set on the slab |
| $x_i$ | building block row element of $\mathbf{U}$ |
| $\mathbf{Y}_j$ | column element group |
| $y$ | co-ordinate set on the slab |
| $y_j$ | building block row element of $\mathbf{V}$ |

*Greek symbols*

| | |
|---|---|
| $\lambda^{(k)}$ | $k$th eigenvalue |
| $\rho_Z$ | contribution of parameter $Z$ to heat transfer performance, $Z$ being any of geometric parameters ($A$–$B_2$) |
| $\Sigma$ | matrix composed of $\sigma^{(k)}$ and 0 |
| $\sigma^{(k)}$ | square root of $\lambda^{(k)}$ |

*Subscripts*

| | |
|---|---|
| $x$ | $x$-direction |
| $y$ | $y$-direction |

patterns thus created are trees [2,4] and mosaics [3] embedded in a matrix. While these patterns studied in [2–4] are regular patterns having multiple length scales, they are the special cases of fractal geometry.

In general, the fractal geometry allows us to find a certain regularity (self-similarity) in a random geometric topography. Applications of the fractal geometry to the analysis of complex heat transfer systems are envisioned in [5]. The fractal analysis helps to reveal geometric features that cannot be captured by classical statistical analysis, but it still needs a large body of geometric data to make the revealed self-similarity statistically meaningful. In other words, when applied in the analysis of heat transfer in composite systems, the constituents (discrete media in a matrix or structural components) of the system must be present in large number in the system's expanse.

The above quick overview of the existing methodologies is presented in order to highlight a geometric feature of complex heat transfer systems considered in the present study. That is, the constituents of the composite system are neither microscopic compared to the system's dimensions nor exist in a large number in the spatial expanse of interest. Instead, their sizes typically range from about one-tenth to several-tenths of the system's dimension. Where the constituents are discrete media or structural components, their population in the space of interest is utmost one hundred. As such, the geometric data contained in an individual system is small, barring the application of statistical or fractal analysis to characterization of the geometric features. Meanwhile, the placement of constituents has a wide range of possibility, so that the entire ensemble of possible system organizations is huge. Although heat transfer in each system organization can be analyzed using an available means, most commonly a numerical simulation code, it is impractical to visit all points in the ensemble by repeated applications of a deterministic method.

Examples of complex systems of the present category are abundant. Typical ones are found in electronic equipment where components of various sizes are packed in a system box. Also, electronic components such as wiring substrates have internal organizations that are categorized as complex systems of the present kind. Indeed, geometric complexity is looming as one of the major challenges to designers of electronic equipment [6]. Today, computational fluid dynamics (CFD) codes are the popular means of thermal design of electronic

equipment. While the CFD code produces detailed solutions of thermal field, its repeated usage for an entire ensemble of design options is time consuming and demands large human and computer resources. Due to geometric complexity of the system's internal organization the productivity of CFD-based design is currently very low. Improvement of designer's productivity is an industry-wide agenda, and the development of a methodology to expedite the analytical work is urgently needed [7].

In a methodology proposed by the present author there are a few key steps [7]. For the purpose of illustration we consider an ensemble of systems where the system's outer dimension is fixed and the components of specified sizes can be placed arbitrarily in the system space. In the first step, we choose a sample design of component placement and perform heat transfer analysis on the sample. Then, create a certain number of variants from the first sample, and perform heat transfer analyses on that set. From the solution body thus developed we deduce the sensitivity of temperature distribution to the component placement pattern. Knowledge about such sensitivity is then incorporated in a simple code that is designed to expedite the analysis. For example, when the component placement pattern in one corner of the system is found not to affect the temperature of a component of primary interest in another corner, components in the former corner are treated in an expeditious code as a lump without regard to their specific arrangement. The entire process that culminates in the production of an expeditious code is named 'Build-up approach (BUA)' to symbolize the development of a knowledge super-layer (expeditious code) on the base of detailed solutions [7]. A full account of the BUA is beyond the scope of the present paper. The above reference to BUA is only to explain the immediate motivation of the present study.

One of the key steps in BUA is the assumption of a set of variants from a sample geometric system. The variants are called here template models. We need a tool to create a set of template models in an organized manner. Such a tool must capture the level of geometric complexity in terms of some quantitative measures. Quantitative analysis of geometric configurations gives us the following practical benefits. It allows us to create a template set where all geometric patterns are at an equal level of complexity. Constituents of the system can be repositioned without affecting the complexity level, and the effects of constituent relocation on the temperature field can be studied. In such a search for better or optimum constituent location, we can use the existing optimization algorithms once we have a means to change the geometric configuration in an organized manner. We can also create models having different levels of complexity, and compare their heat transfer performance. If we find little difference in heat transfer performance between two models, we will choose a simpler model and create its variants for further exploration of the heat transfer versus the geometry, so save time and computational resources. This is tantamount to quantitative organization of geometric modeling.

Within a reasonable writing space it is difficult to cover the whole spectrum of issues involved in quantitative analysis and modeling of geometric configurations. The present paper has an objective of describing only the basics of the proposed methodology. First, it explains the geometric analysis using simple examples that have two-dimensional mosaic patterns of different materials in the slab. Second, it illustrates how the results of geometric analysis can be used to examine the sensitivity of heat transfer performance to the constituent placement in the slab. Also, the search for better constituent placements is discussed.

## 2. Singular-value decomposition analysis

Fig. 1 is an illustration that will be used to explain the geometric data analysis. The patterns in Fig. 1 represent the arrangements of high thermal conductivity material (solid cells) and low conductivity material (open cells) comprising a two-dimensional slab. The patterns of Fig. 1(a) and (b) have an equal number of solid (hence, open) cells. The number of solid cells is 48. Obviously, the pattern of Fig. 1(a) has a much higher level of regularity (lower level of complexity) than that of Fig. 1(b). How can we represent the difference in the two configurations?

The method of our choice is the singular-value decomposition (SVD) of pattern [8]. We view the pattern as a matrix (**S**) of binary digits, representing the solid

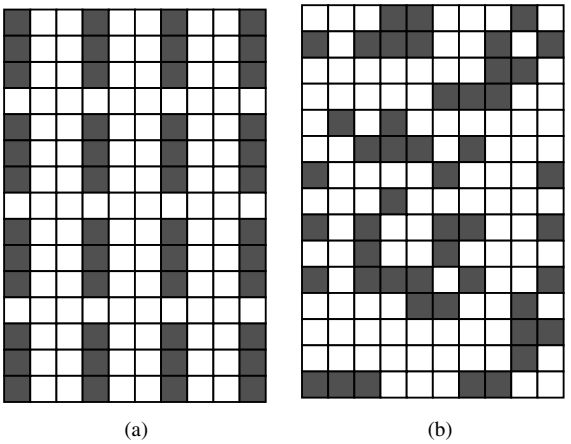


Fig. 1. Patterns having an equal number (48) of solid cells. (a) Regular pattern, (b) arbitrarily created pattern.

cell by '1' and the open cell by '0'. Then, the matrix is decomposed into the left-singular matrix **U** and the right-singular matrix **V**.

$$\mathbf{S} = \mathbf{U}\Sigma\mathbf{V}^{\mathrm{T}}, \tag{1}$$

where

$$\Sigma = \begin{bmatrix} \sigma^{(1)} & 0 & \bullet & \bullet & \bullet & 0 \\ 0 & \sigma^{(2)} & \bullet & \bullet & \bullet & \bullet \\ \bullet & \bullet & \bullet & \bullet & \bullet & \bullet \\ \bullet & \bullet & \bullet & \bullet & \bullet & 0 \\ 0 & \bullet & \bullet & \bullet & 0 & \sigma^{(K)} \end{bmatrix}, \tag{2}$$

$\sigma^{(k)} = \sqrt{\lambda^{(k)}}$, and $\lambda^{(k)}$ is the $k$th eigenvalue determined from

$$\det(\mathbf{S}\mathbf{S}^{\mathrm{T}} - \lambda\mathbf{I}) = 0 \quad \text{for } \mathbf{U}, \tag{3}$$

$$\det(\mathbf{S}^{\mathrm{T}}\mathbf{S} - \lambda\mathbf{I}) = 0 \quad \text{for } \mathbf{V}. \tag{4}$$

$\mathbf{V}^{\mathrm{T}}$ in Eq. (1) is the transpose of **V**, and $\mathbf{S}^{\mathrm{T}}$ in Eqs. (3) and (4) is the transpose of **S**. Eqs. (3) and (4) produce the same unique set of eigenvalues. The eigenvalues are set in decreasing order: $\lambda^{(1)} \geqslant \lambda^{(2)} \geqslant \cdots \geqslant \lambda^{(K)} \geqslant 0$, where $K$ is the number of eigenvalues. Using the eigenvalues we determine the column singular-vectors of **U** from

$$\mathbf{S}\mathbf{S}^{\mathrm{T}}\mathbf{u}^{(k)} = \lambda^{(k)}\mathbf{u}^{(k)} \quad 1 \leqslant k \leqslant K \tag{5}$$

and the normalizing condition

$$\sum_{i=1}^{m} u_{ik}^2 = 1, \tag{6}$$

where $u_{ik}$ is the $i$th element of the $k$th column vector. Likewise, we find the right-singular matrix **V**.

The number of eigenvalues (that is $K$, also the rank of $\mathbf{S}\mathbf{S}^{\mathrm{T}}$ and $\mathbf{S}^{\mathrm{T}}\mathbf{S}$) reflects the complexity of a geometric pattern. The pattern of Fig. 3(a) has one eigenvalue, that is 48 ($\sigma = 6.9282$), a single **U** column vector composed of 0 and 0.2887, and also a single **V** column vector composed of 0 and 0.5. The pattern of Fig. 1(b) has 10 eigenvalues, the maximum being 21.67 and the minimum 0.307, a $15 \times 10$ **U** matrix, and a $10 \times 10$ **V** matrix.

Fig. 2 shows another example, where the number of eigenvalues is five, the maximum eigenvalue being 39.291 and the minimum 0.5516. The number of solid cells is again 48. Fig. 2 includes the full list of matrix elements. Examination of **U** and $\mathbf{V}^{\mathrm{T}}$ reveals that **U** is composed of six distinct row elements, and $\mathbf{V}^{\mathrm{T}}$ is likewise made of six column elements. Among six row or column elements one has only zero elements. An example of non-zero row elements in **U** is [0.3467 0.5357 0.2835 0.0849 0.0726] that appears on the top and the tenth row. An example from $\mathbf{V}^{\mathrm{T}}$ is $[0.1106 \quad 0.5635 \quad 0.3402 \quad 0.1278 \quad 0.1955]^{\mathrm{T}}$ that appears on the second and the third column. These row and column elements, and the eigenvalues or their square roots, are the building blocks of the matrix **S**.

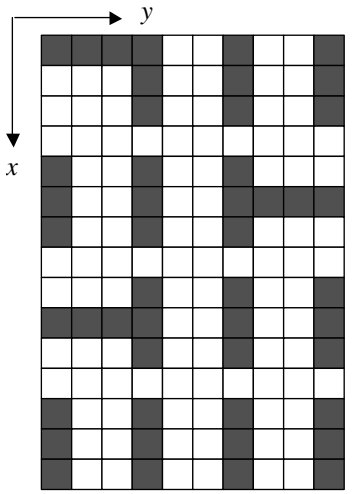


$$\mathbf{U} = \begin{bmatrix}
0.3467 & 0.5357 & 0.2835 & 0.0849 & 0.0726 \\
0.2496 & -0.3119 & 0.2579 & -0.0406 & 0.1493 \\
0.2496 & -0.3119 & 0.2579 & -0.0406 & 0.1493 \\
0 & 0 & 0 & 0 & 0 \\
0.2362 & 0.0743 & -0.4051 & -0.3850 & 0.3554 \\
0.3281 & -0.1277 & -0.4454 & 0.8049 & 0.1729 \\
0.2362 & 0.0743 & -0.4051 & -0.3850 & 0.3554 \\
\mathbf{0} & \mathbf{0} & \mathbf{0} & \mathbf{0} & \mathbf{0} \\
0.2496 & -0.3119 & 0.2579 & -0.0406 & 0.1493 \\
0.3467 & 0.5357 & 0.2835 & 0.0849 & 0.0726 \\
0.2496 & \mathbf{-0.3119} & \mathbf{0.2579} & -0.0406 & 0.1493 \\
\mathbf{0} & \mathbf{0} & \mathbf{0} & \mathbf{0} & \mathbf{0} \\
0.3114 & -0.0570 & -0.1247 & -0.1076 & -0.4538 \\
0.3114 & -0.0570 & -0.1247 & -0.1076 & -0.4538 \\
0.3114 & -0.0570 & -0.1247 & -0.1076 & -0.4538
\end{bmatrix}$$

$$\Sigma = \begin{bmatrix}
6.2683 & 0 & 0 & 0 & 0 \\
0 & 1.9013 & 0 & 0 & 0 \\
0 & 0 & 1.6667 & 0 & 0 \\
0 & 0 & 0 & 1.3282 & 0 \\
0 & 0 & 0 & 0 & 0.7427
\end{bmatrix}$$

$$\mathbf{V^T} = \begin{bmatrix}
0.3874 & 0.1106 & 0.1106 & 0.5467 & 0 & 0 & 0.5467 & 0.0524 & 0.0524 & 0.4713 \\
0.4845 & 0.5635 & 0.5635 & \mathbf{-0.1716} & \mathbf{0} & \mathbf{0} & -0.1716 & -0.0671 & \mathbf{-0.0671} & -0.2498 \\
-0.6377 & 0.3402 & 0.3402 & \mathbf{-0.0188} & \mathbf{0} & \mathbf{0} & \mathbf{-0.0188} & -0.2672 & -0.2672 & 0.4674 \\
-0.0889 & 0.1278 & 0.1278 & \mathbf{-0.2112} & \mathbf{0} & \mathbf{0} & -0.2112 & 0.6060 & 0.6060 & 0.3685 \\
-0.4479 & 0.1955 & 0.1955 & 0.3559 & 0 & 0 & 0.3559 & 0.2327 & \mathbf{0.2327} & -0.6010
\end{bmatrix}$$

Fig. 2. A starter pattern and its matrixes $(\mathbf{U}, \mathbf{V})$ of singular vectors and eigenvalue matrix $(\Sigma)$.

Table 1
Eigenvalues and building block elements of the starter pattern of Fig. 2

*Eigenvalues*
$\lambda^{(1)} = 3.9291\text{E}01$
$\lambda^{(2)} = 3.6151\text{E}00$
$\lambda^{(3)} = 2.7779\text{E}00$
$\lambda^{(4)} = 1.7642\text{E}00$
$\lambda^{(5)} = 5.5164\text{E}{-}01$

*Building blocks for* **U**
$x_0$: 0, 0, 0, 0, 0
$x_1$: 0.34674, 0.53566, 0.28349, 0.08488, 0.07260
$x_2$: 0.24963, −0.31186, 0.25787, −0.04061, 0.14926
$x_3$: 0.23624, 0.07433, −0.40513, −0.38502, 0.35538
$x_4$: 0.32814, −0.12767, −0.44537, 0.80486, 0.17285
$x_5$: 0.31144, −0.05704, −0.12472, −0.10757, −0.45383

*Building blocks for* **V**
$y_0$: 0, 0, 0, 0, 0
$y_1$: 0.38741, 0.48450, −0.63707, −0.08895, −0.44793
$y_2$: 0.11063, 0.56346, 0.34018, 0.12781, 0.19550
$y_3$: 0.54671, −0.17159, −0.01878, −0.21123, 0.35594
$y_4$: 0.05235, −0.06715, −0.26722, 0.60596, 0.23272
$y_5$: 0.47134, −0.24977, 0.46736, 0.36852, −0.60101

Table 1 summarizes the building block elements for a pattern of Fig. 2, where the symbols for the building blocks $x_i$ $(0 \leqslant i \leqslant 5)$ and $y_j$ $(0 \leqslant j \leqslant 5)$ are defined.

Now we can create variants from the pattern of Fig. 2 by relocating $x_i$'s and $y_j$'s in **U** and **V** keeping $\Sigma$ intact. All these patterns are 'geometrically equivalent'; they have the same $\Sigma$ matrix and made of the same building blocks. But, the number of variants is astronomical as readily estimated from permutations of $x_i$'s and $y_j$'s. For example, the building blocks to fill 15 slots of **U** are $3 \times x_0$, $2 \times x_1$, $4 \times x_2$, $2 \times x_3$, $1 \times x_4$, $3 \times x_5$, so the number of permutations amounts to 378,378,000. When multiplied by the number from **V**, the total number of possible configurations becomes $8.5816 \times 10^{13}$!! Obviously, we need to introduce some means to reduce the computational burden. But, before proceeding to tackle this issue, we formulate a heat conduction problem in the next section.

## 3. Heat conduction in slabs

Fig. 3 shows one of the patterns generated by relocating the building blocks of the pattern of Fig. 2. The slab has an outer dimension $L_x \times L_y$, and we assume a unit depth normal to the paper. The open cell (square) has a thermal conductivity $k_0$ and the solid cell (also, square) has $k_1$ We consider steady heat conduction problems where the boundary temperatures are specified uniformly on either the vertical sides ($x = 0$ and $L_x$) or the horizontal sides ($y = 0$ and $L_y$). The remaining sides are adiabatic, so the primary heat

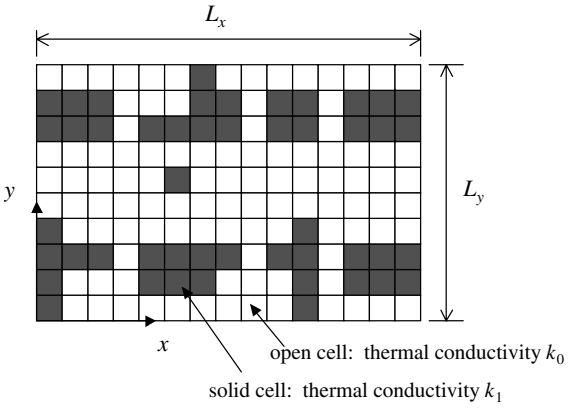


Fig. 3. A slab composed of low (open cell) and high (solid cell) conductivity materials.

flow is in the $x$-direction, or in the $y$-direction. Taking the boundary temperature difference as a temperature scale and $L_y$ as a length scale, we non-dimensionalize the heat conduction equation. In the non-dimensional equation the ratio $(k_1/k_0)$ is a sole property parameter. The non-dimensional equation is solved numerically dividing the zone into $30 \times 20$ meshes (staggered for temperature nodes and heat flow nodes). The meshes are considered fine enough for the present purpose, and the convergence of solution is judged by a criterion that the heat flows on the boundaries are balanced within 0.1% of error. The formulation of finite difference equations and the numerical solution scheme are standard ones, so they need not be reproduced here.

The result of our interest is the equivalent thermal conductivity: it is defined in terms of the dimensional quantities (on the right-hand side) as

$$k_{\mathrm{e},i} \equiv \frac{Q_i L_i}{k_0 \Delta T L_j \cdot 1} \tag{7}$$

where $Q$ is the heat flow rate, $\Delta T$ is the temperature difference between the opposing boundaries of the slab, the suffix $i$ denotes the direction of the primary heat flow ($x$ or $y$) and $j$ is the direction orthogonal to the direction specified by $i$ ($y$ or $x$), and 1 in the denominator means unit slab thickness. Note that the nominal heat flux is $Q_i/(L_j \times 1)$. The 'equivalent thermal conductivity' here does not mean homogenizing the slab's internal organization; it is used merely as a measure of heat transfer performance that is affected by the placement of solid cells.

## 4. Overall plan of analysis

A strategic plan is required to navigate through a vast variant ensemble to explore the relationship

between the heat transfer performance and the solid cell placement. There are an array of methods that have been applied to heat transfer problems involving many parameters and uncertainties; the information measure theory [9], the genetic algorithms (GAs) [10–12], the surrogate model [13], the Monte Carlo, the descriptive, and the gradient methods [14]. The power of each method depends on the nature of problem and the objective of analysis. In many cases the combination of different methods works with a higher efficiency in terms of the time to reach a solution than a single method. There is in fact no universally applicable specific guide about which method or what combination of methods could have the highest efficiency in solution search. Much depends on the hunch of the strategy planner. So, the plan described below does not claim any universality, but grew from the need to acquaint possible users of the methods with the basic concepts of solution search.

Fig. 4 describes the steps comprising the present scheme. The objective here is to find a better placement of solid (highly conductive) cells that produces a higher equivalent thermal conductivity. In the pattern analysis phase we start with the SVD analysis of a sample pattern, then, find the eigenvalues and the building block elements described in Section 2. In the planning phase some of the building blocks are grouped. By grouping, permutations of building block elements are allowed only within the group boundaries. The grouping can be done referring to constraints on component placements in actual systems. For example, in electronic equipment, some components need to be held close together as a group.

Although this grouping significantly reduces the template population, the number of possible templates is likely to remain prohibitive. We then employ the Taguchi method [15] for the first stage screening. The objective of the first stage screening is to grasp a coarse but global picture about the sensitivity of heat transfer performance to the element permutations. We denote the element permutations by symbols, and call the symbols the geometric parameters. The geometric parameters serve as the factors, and the states of the parameters as the levels in the Taguchi method. The next section provides some more details of this step.

Manipulation of the geometric parameters creates a set of patterns, and heat transfer analysis is performed on the created patterns. On the body of heat transfer solutions we apply the Taguchi method, find the sensitivity of heat transfer performance to the parameters, and weed out unimportant parameters from the scope of further studies. The template population becomes significantly small after the first stage screening, but it is still too large for heat transfer analyses to be performed on all models included in the template set. In the present study, fine-tuning of optimization is done by an evolutionary search. The process may be categorized as a GA search. The GA is suitable to work with the present parameter types. As will be shown in the following section the geometric parameters can be manipulated by

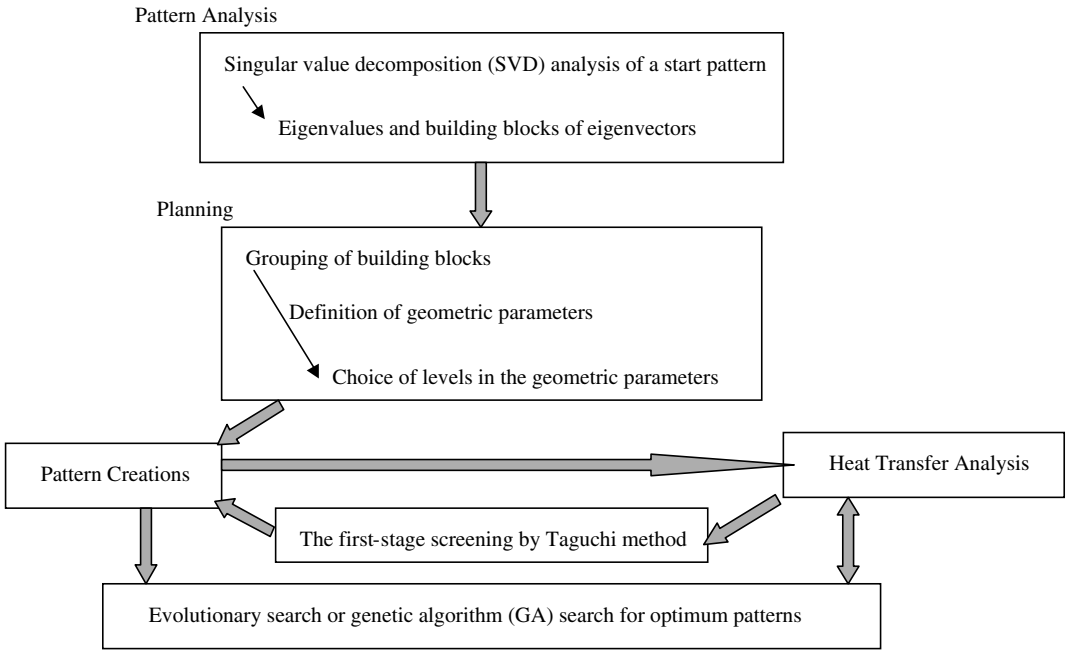


Fig. 4. Steps in hierarchical search for optimum placements of highly conductive cells.

permutation, mutation, and cross-over, namely, the basic operations of GA search.

Although search engines based on the Taguchi method or the GA are commercially available, we resort to hand-on search in the next section. That is, we choose to work on the system of a moderate size and make the search process transparent to those who are not familiar with these search algorithms. One of the important issues in the application of search algorithms is whether the search is trapped in local maximum or minimum before finding a true optimum point. This issue is not included in the following study, as its inclusion duly complicates the search process. For more discussion on the present search scheme, see Appendix A.

## 5. Study on an example ensemble

Our starting point is the pattern of Fig. 2. The building block elements are already listed in Table 1. The building block elements are grouped as shown in Table 2; group $X_1$ is composed of one $x_1$ element and two $x_2$ elements, $X_2$ has one $x_0$, one $x_1$, and two $x_2$ elements, and so on. This grouping is made only to illustrate the process. Arrangements of the groups and the elements within the group are treated as the states of the geometric parameters as shown in Table 2. Parameter $A$ is for the arrangement of $X_i$'s ($i = 1$–4), each arrangement in permutation is a state of $A$. Parameter $B$ has only two states, $(Y_1, Y_2)$ and $(Y_2, Y_1)$. Parameter $A_1$ specifies the arrangement of elements in $X_1$; it has $3!/2! = 3$ states, that is, three ways of permutation for one $x_1$ and two $x_2$ in three slots. $A_2$ has $4!/2! = 12$ states, $A_3$ has 12 states, and so on. The internal organization of $X_4$ is fixed as $(x_0 x_5 x_5 x_5)$. The total number of states of the geometric parameters, that is the total template population, is obtained from the product of states of $A$, $B$, $A_1$ to $A_3$, $B_1$ and $B_2$. The template population thus computed is significantly reduced from the order of $10^{13}$ (Section 2), but still of the order of $10^6$.

In applying the Taguchi method for the first stage screening we pick up two states, or levels in the terminology of the Taguchi method, from the geometric parameters. We set the levels as shown in Table 2. Then, we run the heat conduction solver for eight cases over which two levels (denoted by 1 and 2) of the parameters are distributed as shown in Table 3. Note that each column in the table has four 1s and four 2s. Moreover, to four 1s on any column, there correspond two 1s and two 2s on other columns. The same can be observed for four 2s on any column. So, when the results from runs 1–4 are averaged, the average contains contributions from two levels of the parameters except $A$ whose level is set at 1. The average from runs

Table 2
Grouping of building block elements, geometric parameter symbols, and specifications of levels for the first-stage screening

*Grouping of $x_i$'s and $y_j$'s*
$X_1$: $x_1$, $2 \times x_2$
$X_2$: $x_0$, $x_1$, $2 \times x_2$
$X_3$: $x_0$, $2 \times x_3$, $x_4$
$X_4$: $x_0$, $3 \times x_5$
$Y_1$: $y_0$, $y_1$, $2 \times y_2$, $y_3$
$Y_2$: $y_0$, $y_3$, $2 \times y_4$, $y_5$

*Geometric parameters*
$A$: Arrangement of blocks $(X_1, X_2, X_3, X_4)$
$B$: Arrangement of blocks $(Y_1, Y_2)$
$A_1$: Arrangement of $(x_1, 2 \times x_2)$ in $X_1$
$A_2$: Arrangement of $(x_0, x_1, 2 \times x_2)$ in $X_2$
$A_3$: Arrangement of $(x_0, 2 \times x_3, x_4)$ in $X_3$
$B_1$: Arrangement of $(y_0, y_1, 2 \times y_2, y_3)$ in $Y_1$
$B_2$: Arrangement of $(y_0, y_3, 2 \times y_4, y_5)$ in $Y_2$

*Definition of levels*

| Parameter | Level 1 | Level 2 |
|---|---|---|
| $A$ | $X_1 X_3 X_2 X_4$ | $X_1 X_4 X_2 X_3$ |
| $B$ | $Y_1 Y_2$ | $Y_2 Y_1$ |
| $A_1$ | $x_1 x_2 x_2$ | $x_2 x_1 x_2$ |
| $A_2$ | $x_0 x_2 x_1 x_2$ | $x_2 x_0 x_2 x_1$ |
| $A_3$ | $x_0 x_3 x_4 x_3$ | $x_0 x_3 x_3 x_4$ |
| ($X_4$ is fixed as $x_0 x_5 x_5 x_5$) | | |
| $B_1$ | $y_1 y_2 y_2 y_3 y_0$ | $y_2 y_1 y_3 y_2 y_0$ |
| $B_2$ | $y_0 y_3 y_4 y_4 y_5$ | $y_4 y_0 y_3 y_5 y_4$ |

Table 3
Plan of numerical analysis runs: Levels of $A$–$B_2$ are specified by 1 and 2

| Run no. | $A$ | $B$ | $A_1$ | $A_2$ | $A_3$ | $B_1$ | $B_2$ |
|---|---|---|---|---|---|---|---|
| 1 | 1 | 1 | 1 | 1 | 1 | 1 | 1 |
| 2 | 1 | 1 | 1 | 2 | 2 | 2 | 2 |
| 3 | 1 | 2 | 2 | 1 | 1 | 2 | 2 |
| 4 | 1 | 2 | 2 | 2 | 2 | 1 | 1 |
| 5 | 2 | 1 | 2 | 1 | 2 | 1 | 2 |
| 6 | 2 | 1 | 2 | 2 | 1 | 2 | 1 |
| 7 | 2 | 2 | 1 | 1 | 2 | 2 | 1 |
| 8 | 2 | 2 | 1 | 2 | 1 | 1 | 2 |

5–8 contains contributions from two levels of the parameters except $A$ whose level is set this time at 2. Hence, the difference between the average from runs 1–4 and that from 5–8 tells how influential $A$ is. Likewise, the influences of other parameters on the heat transfer performance can be estimated by comparing two averages from runs for 1s and 2s on the column. By substituting $-1$ for 1 and 1 for 2 in Table 3 we note that any pair of columns satisfies the orthogonality condition, that is, the sum of element pairs on two columns is zero.

Table 4 summarizes the results of numerical analysis in terms of the equivalent thermal conductivity $k_{e,x}$ and $k_{e,y}$ for the cases of $k_1/k_0 = 100$, 10, and 2. The equivalent thermal conductivity in the $x$-direction, $k_{e,x}$ is higher than that in the $y$-direction, $k_{e,y}$, for all three cases of $k_1/k_0$. This reflects the effects of element grouping that tends to leave strips of solid cells elongated in the $x$-direction. However, the difference between $k_{e,x}$ and $k_{e,y}$ diminishes as $k_1/k_0$ decreases, because the thermal resistance by the open cells come to predominate. Using these results we estimate the contributions from $A$–$B_2$ to the heat transfer performance of the slab as follows. We use the results of $k_{e,x}$ for $k_1/k_0 = 100$ as an example.

(1) Compute the column average,

$$\overline{k_{e,x}} = \frac{1}{8}\sum_{\text{col}} k_{e,x}, \tag{8}$$

where the summation is taken over the column, that is, over the results of run 1–8.

(2) Compute the deviation from the column average for $k_{e,x}$ of each run

$$\Delta k_{e,x} = k_{e,x} - \overline{k_{e,x}}. \tag{9}$$

(3) The effect of $A$ on $k_{e,x}$ is computed as

$$S_A = \frac{((\text{average } \Delta k_{e,x} \text{ for run 1–4}) - (\text{average } \Delta k_{e,x} \text{ for run 5–8}))^2}{8 \times \left(\frac{1}{4}\right)^2}, \tag{10}$$

where the denominator on the right-hand side is a factor introduced to account for the data population involved in the computation. Since it is cancelled out in later computations, the detailed account about this factor is saved. The effect of $B$ on heat transfer performance, $S_B$ is computed using the average $k_{e,x}$ from runs 1, 2, 5, 6 and that from runs 3, 4, 7, 8; the effect of $A_1$, $S_{A_1}$ using the average $k_{e,x}$ from runs 1, 2, 7, 8 and that from 3, 4, 5, 6; and so on.

(4) Contribution from $A$ to $k_{e,x}$ is computed as

$$\rho_A = S_A/(S_A + S_B + S_{A_1} + S_{A_2} + S_{A_3} + S_{B_1} + S_{B_2}). \tag{11}$$

Table 4
Computed equivalent thermal conductivity values

| Run no. | $k_1/k_0 = 100$ | | $k_1/k_0 = 10$ | | $k_1/k_0 = 2$ | |
|---|---|---|---|---|---|---|
| | $k_{e,x}$ | $k_{e,y}$ | $k_{e,x}$ | $k_{e,y}$ | $k_{e,x}$ | $k_{e,y}$ |
| 1 | 3.142 | 2.807 | 2.197 | 1.864 | 1.267 | 1.233 |
| 2 | 3.142 | 2.306 | 2.204 | 1.776 | 1.268 | 1.231 |
| 3 | 3.094 | 2.055 | 2.193 | 1.736 | 1.268 | 1.231 |
| 4 | 3.490 | 2.522 | 2.309 | 1.834 | 1.272 | 1.232 |
| 5 | 3.147 | 2.413 | 2.191 | 1.805 | 1.267 | 1.233 |
| 6 | 3.283 | 2.413 | 2.234 | 1.812 | 1.269 | 1.233 |
| 7 | 3.325 | 2.117 | 2.266 | 1.737 | 1.272 | 1.230 |
| 8 | 3.028 | 2.165 | 2.160 | 1.752 | 1.262 | 1.227 |

Contributions from the remaining parameters are computed similarly.

A summary of the contributions is given in Table 5. The contribution of a parameter depends on the primary direction of heat flow and $k_1/k_0$ Interpretation about the behavior of parameter contributions is not attempted here for the sake of brevity. The point is that we identify a few influential parameters from this table. To illustrate the step of improving the heat transfer performance we take up the case of $k_{e,x}$ and $k_1/k_0 = 100$ as an example.

From Table 5, we take $A_3$ and $B_2$ as variables because of their large contributions. Other parameters are fixed as shown in Table 6. The template population is now drastically reduced, but it is still 720 (12 permutations in $X_3$ and 60 permutations in $Y_2$). We first pick up four sets of $A_3$- and $B_2$-states at random as shown in the first

Table 5
Contributions from the parameters to the equivalent thermal conductivity (in percentage)

| | $k_1/k_0 = 100$ | $k_1/k_0 = 10$ | $k_1/k_0 = 2$ |
|---|---|---|---|
| *Primary heat flow in the x-direction ($k_{e,x}$)* | | | |
| $\rho_A$ | 0.6 | 2.1 | 4.4 |
| $\rho_B$ | 4.0 | 8.0 | 1.6 |
| $\rho_{A_1}$ | 11.3 | 7.7 | 8.6 |
| $\rho_{A_2}$ | 4.4 | 2.8 | 1.6 |
| $\rho_{A_3}$ | 24.8 | 26.7 | 29.8 |
| $\rho_{B_1}$ | 0.1 | 1.2 | 14.3 |
| $\rho_{B_2}$ | 54.8 | 51.4 | 39.7 |
| *Primary heat flow from in the y-direction ($k_{e,y}$)* | | | |
| $\rho_A$ | 10.0 | 8.7 | 6.8 |
| $\rho_B$ | 34.4 | 31.6 | 42.4 |
| $\rho_{A_1}$ | 0 | 2.7 | 27.1 |
| $\rho_{A_2}$ | 0 | 0.8 | 6.8 |
| $\rho_{A_3}$ | 0.2 | 0.1 | 1.7 |
| $\rho_{B_1}$ | 30.4 | 30.4 | 0 |
| $\rho_{B_2}$ | 25.0 | 25.6 | 15.3 |

Table 6
Evolutionary search for patterns producing higher equivalent thermal conductivity; focus on the effects of $A_3$ and $B_2$ on $k_{e,x}$ for $k_1/k_0 = 100$

*Fixed*
$A$ at level 1: $X_1 X_3 X_2 X_4$
$B$ at level 2: $Y_2 Y_1$
$A_1$ at level 2: $x_2 x_1 x_2$
$A_2$ at level 2: $x_2 x_0 x_2 x_1$
$B_1$ at level 1: $y_1 y_2 y_2 y_3 y_0$

| Run no. | $A_3(X_3)$ | $B_2(Y_2)$ | $k_{e,x}$ |
|---|---|---|---|
| *First generation* | | | |
| E-1 | $x_0 x_3 x_3 x_4$ | $y_0 y_3 y_4 y_4 y_5$ | 3.490 |
| E-2 | $x_0 x_4 x_3 x_3$ | $y_0 y_5 y_4 y_3 y_4$ | 3.422 |
| E-3 | $x_4 x_3 x_0 x_3$ | $y_5 y_4 y_3 y_4 y_0$ | 3.288 |
| E-4 | $x_3 x_3 x_0 x_4$ | $y_4 y_4 y_0 y_5 y_3$ | 3.004 |
| *Second generation* | | | |
| E-5 | $x_0 x_3 x_3 x_4$ | $y_0 y_3 y_4 y_4 y_5$ | 3.490 |
| E-6 | $x_0 x_3 x_3 x_4$ | $y_0 y_5 y_4 y_3 y_4$ | 3.400 |
| E-7 | $x_0 x_4 x_3 x_3$ | $y_0 y_3 y_4 y_4 y_5$ | 3.578 |
| E-8 | $x_0 x_3 x_3 x_4$ | $y_0 y_3 y_5 y_4 y_4$ | 3.207 |
| *Third generation* | | | |
| E-9 | $x_0 x_4 x_3 x_3$ | $y_0 y_3 y_4 y_4 y_5$ | 3.578 |
| E-10 | $x_3 x_3 x_0 x_4$ | $y_0 y_3 y_4 y_4 y_5$ | 3.495 |
| E-11 | $x_3 x_3 x_4 x_0$ | $y_0 y_3 y_4 y_4 y_5$ | 3.577 |
| E-12 | $x_3 x_4 x_3 x_0$ | $y_0 y_3 y_4 y_4 y_5$ | 3.488 |

generation, E-1 to E-4, in Table 6. By numerical analysis we find the values of $k_{e,x}$, that of E-1 being the highest and that of E-2 the second highest. Following the survival-of-the-fittest rule of GA we preserve the $X_3$ feature of E1 in three templates (E-5, E-6, E-8) of the second generation, and that of E-2 in E-7. E-5 is a copy of E-1. The arrangement in $Y_2$ of E-6 is brought over from E-2. Since $X_3$ of E-6 is $X_3$ of E-1, this is tantamount to a blockwise swapping on E-1 and E-2, $X_3$ of E-1 to that of E-2, to produce E-6. Also, blockwise swapping, $X_3$ of E-2 to that of E-1 while preserving $Y_2$ of E-1, produces E-7. In $Y_2$ of E-8, the head ($y_0$) and the tail ($y_5$) are preserved from $Y_2$ of E-2, but the internal arrangement of E-2 ($y_5 y_4 y_3$) is subjected to cyclic cross-over [16]. We hit upon the highest $k_{e,x}$ in E-7, so E-7 is copied in E-9 of the third generation. In the third generation, $Y_2$ is held intact, and only the elements of $X_3$ are shuffled. Examination of the $k_{e,x}$ values from the first to the third generation indicates that further search may produce only marginal improvement in $k_{e,x}$.

Fig. 5 shows samples of patterns and computed temperature distributions. To aid the visual examination the grids are shown in both the pattern diagrams (on the left) and the temperature diagrams (on the right), with the grid density in the latter doubled from that of the former. The pattern at the top is that of Fig. 2 (note the rotation of the drawing by 90° as indicated by the symbols of the coordinate axes), that in the middle is a pattern of E-1, and that at the bottom is a pattern of E-9 (E-7). The temperature is normalized by $\Delta T$, hence, $T = 1$ on the left boundary and 0 on the right. The temperature distribution is shown in incremental normalized scales. The scales are listed on the right of each temperature distribution diagram. The ranges from the top to the bottom in the list correspond to the bands from the left to the right in the temperature distribution diagram, the highest range 0.9–1 corresponding to the leftmost band, and the lowest range 0–0.1 to the rightmost band. The isotherms imply complex heat flow patterns resulted from the locations of the vertical and

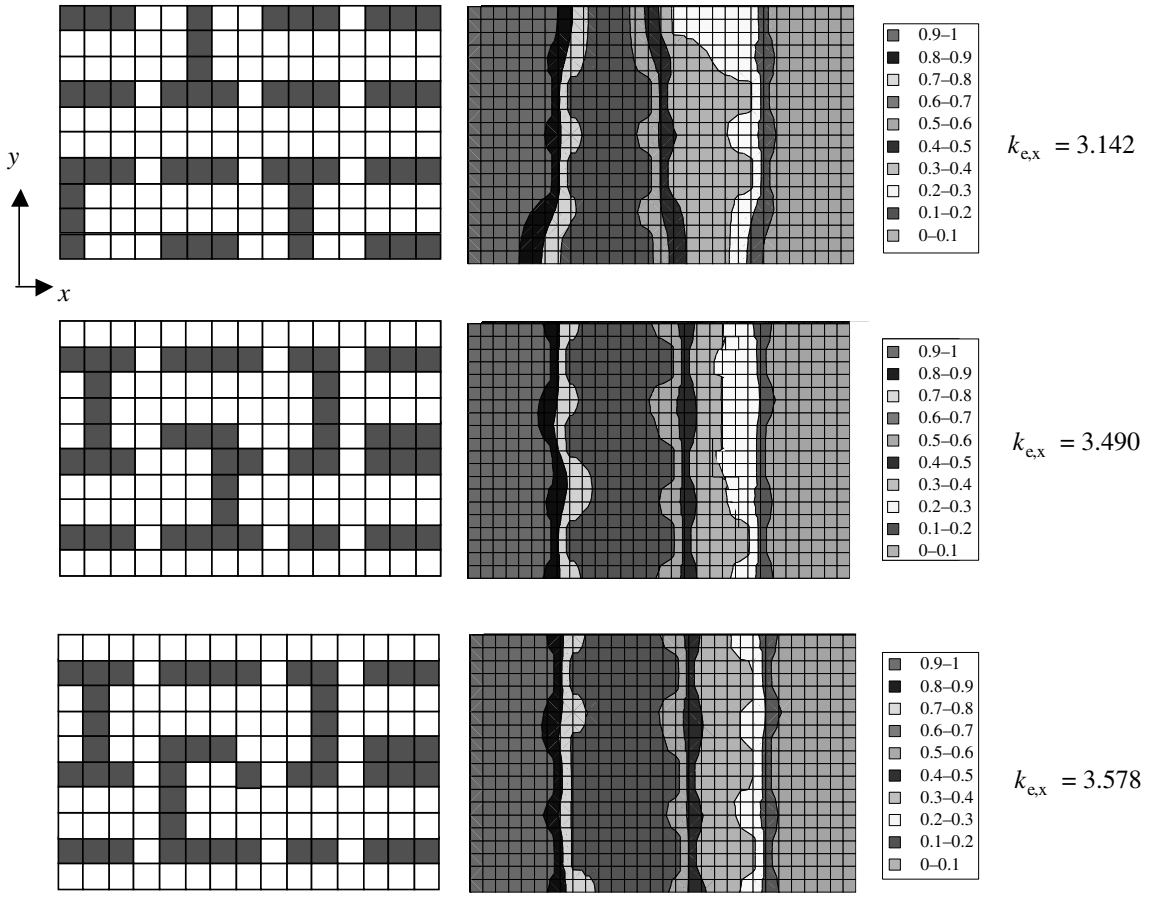


Fig. 5. Patterns sampled from the variant set and temperature distributions ($k_1/k_0 = 100$). The temperature (normalized) at the left edge of the slab is 1, that at the right edge is 0, and the upper and lower edges are adiabatic.

horizontal conductive strips. However, some generic observations can be drawn from these examples. Observing from the top to the bottom temperature diagrams we find the isotherms coming more aligned to the $y$-axis. Skewed isotherms (sloped against the $y$-axis) mean longer heat flow paths from the left edge to the right, of course, in certain average sense. From the top diagram to the middle, the equivalent thermal conductivity is raised by 11%. Improvements of the isotherm pattern from the middle diagram to the bottom seem small, actually bringing a 2.5% upgrading to the equivalent thermal conductivity.

## 6. Conclusions

Knowledge about the sensitivity of heat transfer performance to the constituent arrangement in a composite system leads us to a design of better internal organization of the system. However, where the constituent arrangement in the system space has a large degree of freedom, we have to resolve two issues. One is the complexity of heat flow paths resulted from geometrically complex arrangements of constituents, and the other is the requirement on computational resources that grows prohibitively large due to a vast number of possible constituent placements. The present paper proposed a methodology whereby these issues are addressed in a systematic manner. Its key ingredients and the conclusions are enumerated as follows.

(1) The constituent placement is captured as a two-dimensional pattern of solid cells representing material of high thermal conductivity embedded in a matrix of low thermal conductivity. On a pattern assumed as a starter, the SVD analysis is performed, and from the sets of left-singular vectors and right-singular vectors the building block elements of the pattern are identified.

(2) By shuffling the building block elements a set of variants from the starter pattern are created. Heat transfer analysis is performed on sample patterns picked up from the ensemble of variants. In the first-stage screening by the Taguchi method, the arrangements of groups of building block elements, and the arrangements of building block elements in the groups are treated as levels taken by the geometric parameters. Influential blocks of elements are identified from the heat transfer solutions on the sampled variants.

(3) A basic version of GAs is applied to the analysis on a body of constituent patterns that have already been narrowed down by the first stage screening. The whole steps from the SVD analysis to the identification of better constituent arrangements are demonstrated on the problem of heat conduction through composite slabs.

(4) The SVD analysis provides a means to change the constituent placement in a manner adaptable to the existing search algorithms for better or optimum placements.

(5) The SVD analysis also leads to the development of a systematic way of modeling complex systems, neglecting unimportant details, thereby, assuming simpler models than actual systems. Discussion of this benefit and applications of the present methodology to other systems such as electronic equipment is left to future reports.

## Acknowledgements

The present study is a part of the project 'RC202 Studies on Reliability of Electronic Devices/Electronic Packaging' that is in progress under the auspices of the Computational Mechanics Division, the Japan Society of Mechanical Engineers. The author wishes to thank for the support rendered through this JSME project.

## Appendix A

This appendix provides supplementary information on the optimization methods employed in the present study and the idea behind the example problem.

The Taguchi method was originated from statistical quality control of industrial products. It is a tool to estimate the sensitivity of product quality to multiple parameters involved in the manufacturing process. In recent years its application has been extended beyond the quality control field to other engineering and research practices. See, for example, [17,18]. The primary function of the Taguchi method is the screening of relevant parameters rather than pinpoint optimization. Contributions of the parameters to the end result (sensitivity measures) are computed, and those having low percentage points are discarded from the list of control parameters. A key element of the Taguchi method is a table of parameter levels that is designed to reduce the requirement for experimental or computational runs. This and other elements of the Taguchi method are described in Section 5.

Creation of a parameter-levels table in the Taguchi method involves certain ad hoc exercises. The 'orthogonality condition' (the end of the second paragraph of Section 5) that needs to be materialized in the table is a constraint on the coverage of parametric domain. The most elementary form is composed of seven parameters and two levels (Table 3 of Section 5). As the number of parameters and the levels are increased, the table expands and materialization of the orthogonality condition requires tedious checking. Also, one cannot choose the number of parameters and that of levels independently. They are interlocked under the orthogonality condition. (Presently, 11 parameters with two levels plus

12 parameters with three levels constitute a largest table, and a commercial code is available for orthogonality checking.) So, in cases where a large number of parameters are involved, one needs to pick some parameters for the sensitivity study and leave the rest fixed. Setting the parameter values on 'levels', typically on two levels, is also an exercise of ad hoc nature. Where extreme values in a parametric range are obvious, they are natural choices. In general, the level setting is an artwork largely based on one's insight and experience. The level setting affects the conclusion; where they are set by a too narrow separation, the parameter effect tends to be underestimated. Naturally, there remains a sense of uncertainty as to the relative importance of untested (fixed) parameters and the correctness of level setting. In theory, one can reduce the uncertainties by iterative selection of the parameters and re-setting of the levels. In so doing, one can also narrow down a range of optimum parameter values. However, the entire process is hard to be automated, so, the Taguchi method yields to the GA as a tool for pinpoint optimization.

The GA has been developed by now to be a robust tool of optimization. Use of the GA from the outset, skipping the screening by the Taguchi method, is in principle possible. One may even construct a process of multi-stage search using the GA alone, starting with global screening and ending with pinpointing an optimum parametric combination. The choice of the optimization process, either serial applications of the Taguchi method and the GA or the GA alone, is essentially a matter of one's preference. In the present study, the Taguchi method is incorporated in the search process favoring its capability to produce quantitative information regarding the parameters' relative importance. Such information does not necessarily clearly emerge from a result of GA search alone.

Both the Taguchi method and the GA can deal with parameters that are hard to be described in conventional quantitative terms. Component placement pattern studied in the present paper is one of such parameters. A parameter needs to be represented by a string of symbols or numerals in the Taguchi method or the GA. In the present study, symbol strings are created from the SVD analysis of component placement patterns. Of course, the SVD analysis is not a sole means of string creation. See [10–12] for other examples of string creation. Further discussions on the issue of parameter representation are saved for future publications currently in preparation.

Finally, a note is made about grouping and permutations of the singular vector elements (or cells after pattern construction by Eq. (1)) in the example problem of Section 5. By grouping one defines a length scale of shuffling, that is the scale over which the grouped cells move around in permutation. Where the groups are packed in a domain, the shuffling length scale is equal to a representative group size. Grouping defined in Table 2 defines a shuffling length of about a quarter (half) of the longer (shorter) side of the domain rectangle. Permutation of elements in the groups is a shuffling in finer length scales. Thus, the grouping is a step in the multi-stage search on the shuffling length scale. In the example problem, the block elements of singular vectors are grouped such that, when a pattern is constructed using Eq. (1), the cells are nearly evenly assigned to six block zones in all group permutations. The group size is a strategic factor that affects the search process. Where only a few groups are defined in the domain, all permutations of the groups can be studied without resorting to samplings of the Taguchi method or the GA. On the other hand, a reduced-size group allows the study of all permutations of elements in the group. In either case, samplings are applied, to element permutations in the group or permutations of fine and numerous groups in the domain. The sampling leaves uncertainties as to the effect of unvisited permutations, and iterative search to reduce the uncertainties is generally time consuming. There is a balance point between the cost of search and the level of uncertainty that is to be struck by the definition of group size. For problems such as optimization of components placement in electronic equipment, samplings on both group permutations and elements permutations in the groups is a practical option. In the example problem of Section 5 the number of groups is set at a level that allows the study of all group permutations in a reasonable time frame. However, full coverage of permutations is sidestepped to simulate actual design studies. A guide for sampling and permutations in the example problem, that produced the patterns of Fig. 5, is that the overall geometrical feature does not deviate markedly from those found in the cross-section of printed circuit boards.

## References

[1] P. Furmanski, Heat conduction in composites: homogenization and macroscopic behavior, Appl. Mech. Rev. 50 (6) (1997) 327–356.

[2] A. Bejan, From heat transfer principles to shape and structure in nature: constructual theory, ASME J. Heat Transfer 122 (2000) 430–449.

[3] A.R. Kacimov, Yu.V. Obnosov, Conduction through a grooved surface and Sierpinsky fractals, Int. J. Heat Mass Transfer 43 (2000) 623–628.

[4] Y. Chen, P. Cheng, Heat transfer and pressure drop in fractal tree-like microchannel nets, Int. J. Heat Mass Transfer 45 (2002) 2643–2648.

[5] A. Majumudar, Role of fractal geometry in the study of thermal phenomena, in: C.-L. Tien (Ed.), Annual Review of Heat Transfer, vol. 4, Begell House, Inc., New York, 1991, pp. 51–110.

[6] W. Nakayama, Thermal management of electronic equipment: research needs in the mid 1990s and beyond, ASME Appl. Mech. Rev. 49 (10) Part 2 (1996) S167–S174.
[7] W. Nakayama, An approach to fast thermal design of compact electronic systems: a JSME project, in: Proceedings IPACK'01, The Pacific Rim/ASME International Electronic Packaging Conference and Exhibition, ASME, Kauai, Hawaii, 2001, Paper No. IPACK2001-15532.
[8] M. Kirby, Geometric Data Analysis, John Wiley & Sons, 2001, pp. 51–61.
[9] A.F. Emery, Using the concept of information to optimally design experiments with uncertain parameters, ASME J. Heat Transfer 123 (2001) 593–600.
[10] N. Queipo, R. Devarakonda, J.A.C. Humphrey, Genetic algorithms for thermosciences research: application to the optimized cooling of electronic components, Int. J. Heat Mass Transfer 37 (6) (1994) 893–908.
[11] S. Jain, H.C. Gea, PCB layout design using a genetic algorithm, ASME J. Electron. Packag. 118 (1996) 11–15.
[12] A.J. Scholand, R.E. Fulton, B. Bras, An investigation of PCB layout by genetic algorithms to maximize fatigue life, ASME J. Electron. Packag. 121 (1999) 31–36.
[13] N. Leoni, C.H. Amon, Bayesian surrogates for integrating numerical, analytical, and experimental data: application to inverse heat transfer in wearable computers, IEEE Trans. Components Packag. Technol. 23 (1) (2000) 23–32.
[14] B.A. Cullimore, Dealing with uncertainties and variations in thermal design, in: Proceedings of IPACK'01, The Pacific Rim/ASME International Electronic Packaging Technical Conference and Exhibition, ASME, Kauai, Hawaii, 2001, Paper No. IPACK2001-15516.
[15] G. Taguchi, Systems of Experimental Design: Engineering Methods to Optimize Quality and Minimize Cost, UNIPUB/Kraus International, White Plains, New York, 1987 (The original Japanese 3rd version was published from Maruzen Publishing Company, Tokyo, 1976.).
[16] D.E. Goldberg, Genetic Algorithms in Search, Optimization, and Machine Learning, Addison-Wesley Publishing Company, 1989, pp. 170–171.
[17] Q. Yu, N. Koizumi, H. Yajima, M. Shiratori, Optimum design of vehicle frontal structure and occupant restraint system for crashworthiness, JSME Int. J., Ser. A 44 (4) (2001) 594–601.
[18] Q. Yu, T. Kashiwamura, M. Shiratori, T. Yamada, Optimal and robust design of nonlinear structures under uncertain loads using statistical optimization method, in: S. Hernandez, A.J. Kassab, C.A. Brebbia (Eds.), Computer Aided Optimum Design of Structures VI, WIT Press, Southampton, Boston, 1999, pp. 97–105.